

Spontaneous asymmetrical crystallization of a quartz-type framework from achiral precursors

Wenxu Zheng,^{ab} Yongqin Wei,^a Xueying Xiao,^{ab} and Kechen Wu^{a*}

^a State Key Laboratory of Structure Chemistry, Fujian Institute of Research on the Structure of Matter, Chinese Academy of Sciences, Fuzhou, Fujian 350002, P. R. China

^b Graduate School of Chinese Academy of Sciences, Beijing 100039, P. R. China.

* The corresponding author, Tel: (+86)- 591-83792600; E-mail: wkc@fjirsm.ac.cn

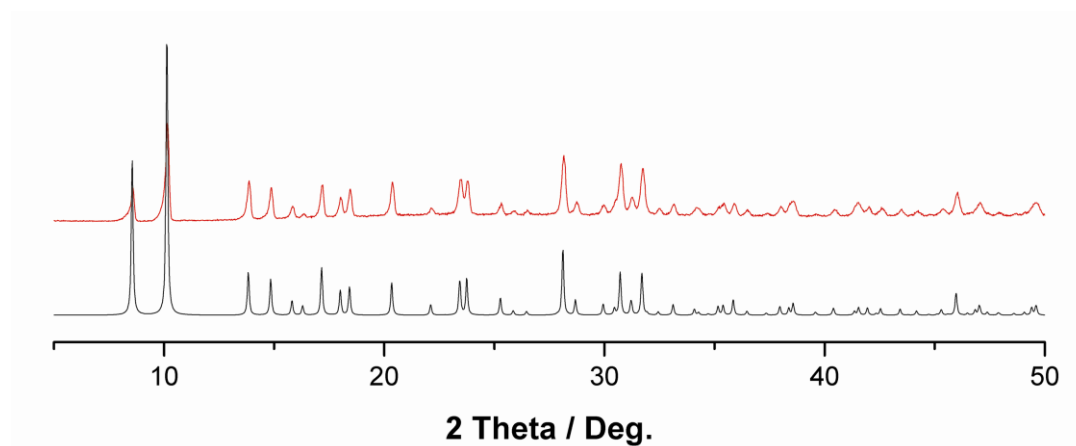


Figure S1. XPRD patterns for **1** (top, red) experimental at room temperature; (bottom, black) calculated on the basis of the structure determined by single-crystal X-ray diffraction.

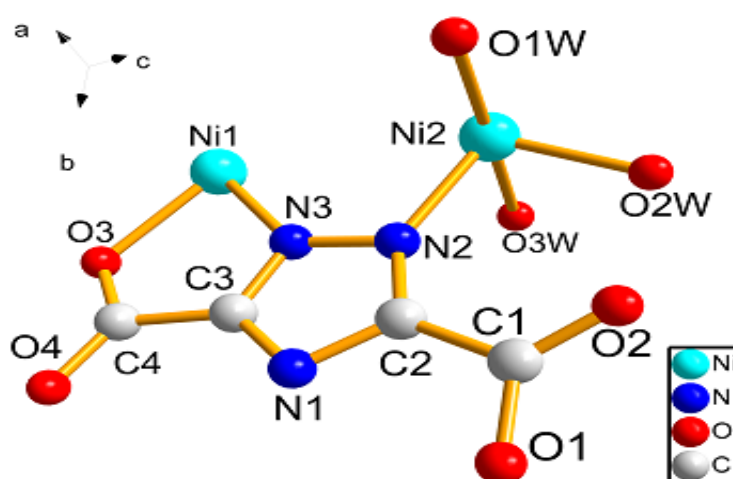


Figure S2. The crystallographic asymmetric unit in compound **1**. Hydrogen atoms are omitted for clarity.

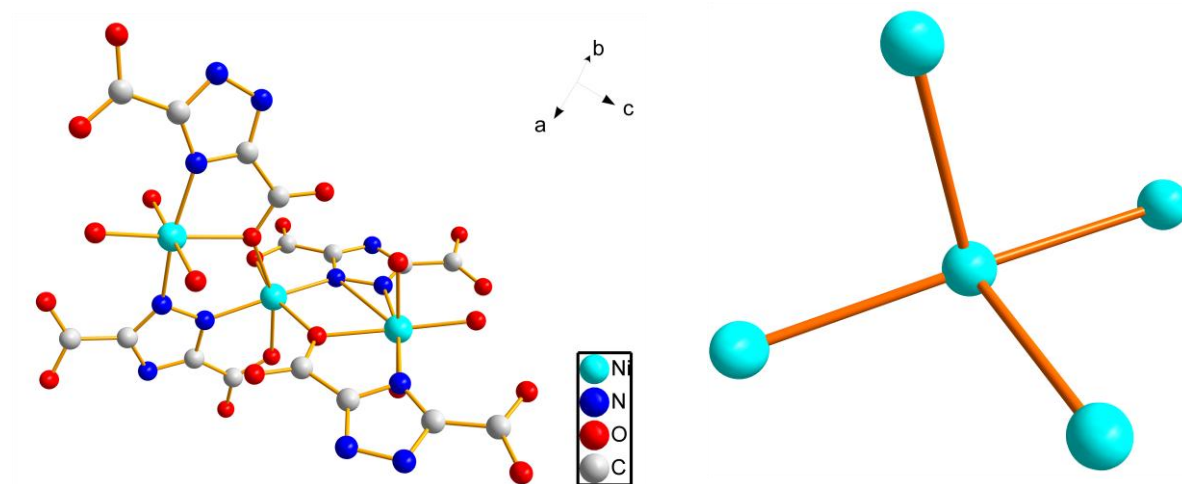


Figure S3. Left: the trinuclear SBU and tetrahedron building block in compound **1**; Right: the node (represent trinuclear SBU) and rod (represent ligand) of topology.

Table S1 A summary of the 10 structure determinations of **1** with the R factors and Flack absolute structure parameters for each refinement.

	Space group	a = b	c	R ₁	wR ₂	Flack parameter
1-1	<i>P</i> 3 ₁ 21	11.92450(10)	16.3020(5)	0.0444	0.1223	0.02(2)
1-2	<i>P</i> 3 ₁ 21	11.9265(5)	16.3060(11)	0.0529	0.1444	0.01(3)
1-3	<i>P</i> 3 ₁ 21	11.910(9)	16.306(13)	0.0556	0.1468	0.02(3)
1-4	<i>P</i> 3 ₁ 21	11.9386(5)	16.2986(15)	0.0958	0.2183	0.01(5)
1-5	<i>P</i> 3 ₁ 21	11.9130(8)	16.2942(19)	0.0898	0.1951	0.01(5)
1-6	<i>P</i> 3 ₁ 21	11.9224(4)	16.2261(11)	0.0657	0.1439	0.03(3)
1-7	<i>P</i> 3 ₁ 21	11.9250(4)	16.2715(10)	0.0401	0.1132	0.01(2)
1-8	<i>P</i> 3 ₁ 21	11.9298(4)	16.4486(8)	0.0527	0.1380	0.03(3)
1-9	<i>P</i> 3 ₁ 21	11.8921(6)	16.248(2)	0.0478	0.1304	0.01(3)
1-10	<i>P</i> 3 ₂ 21	11.9029(6)	16.2687(15)	0.0848	0.2255	0.04(5)

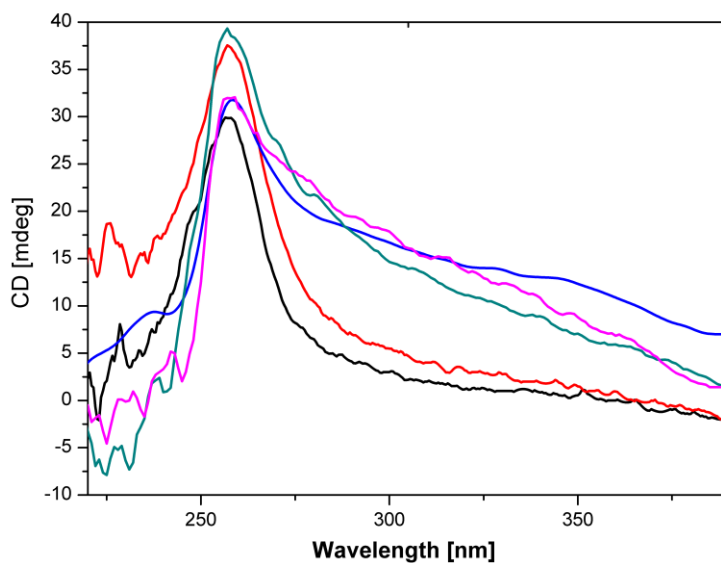


Figure S4. The solid-state CD spectra of each whole batch from 5 parallel products.

CD spectra of each whole batch from 5 parallel hydrothermal syntheses were measured in solid-state. The mixture of 0.6g sample and 1.2g dried KCl powder was grinded for 30 minute, and then 20 mg sample was picked out from the well-ground powder for use in CD measurement.



Figure S5. The image of green products.

Magnetic properties: Magnetic susceptibilities were measured for **1** with a Quantum Design MPMS-XL system.

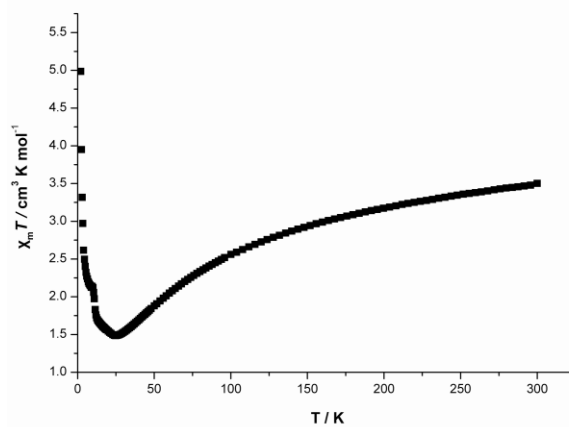


Figure S4. Plot of $\chi_m T$ vs. T for **1** at 1000 oe.

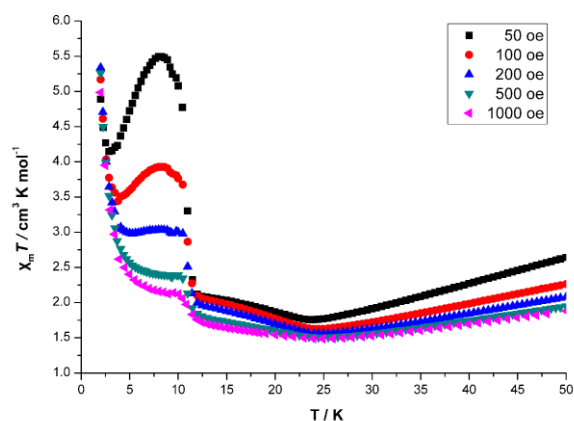


Figure S5. Plot of $\chi_m T$ vs. T under different fields at low temperature.

A plot of $\chi_m T$ vs. T per Ni3 unit under a applied field of 1000 oe for **1** is shown in Figure S1. Upon cooling, the $\chi_m T$ undergoes a gradual decrease down to $1.46 \text{ cm}^3 \text{ K mol}^{-1}$ around 25 K. Below 25 K, the $\chi_m T$ product increases rapidly to a sharp maximum of $4.98 \text{ cm}^3 \text{ K mol}^{-1}$ at 2 K. As shown in Figure S2, the $\chi_m T$ curve is field dependent and disappears at higher field. Such behavior can well be expected for a canted spin system.

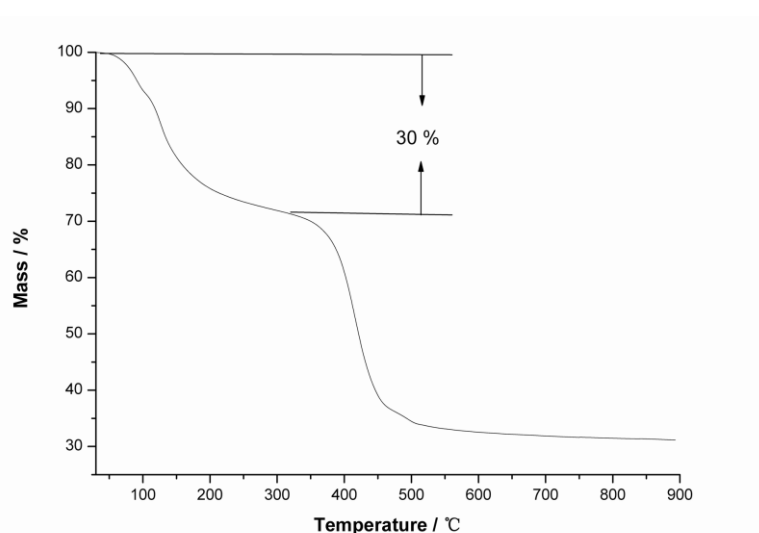


Figure S6. The TGA diagram of **1**. The weight of 30% is corresponding to the loss of uncoordinated and coordinated water molecules.